Available online at www.sciencedirect.com

jmr&t Journal of Materials Research and Technology

journal homepage: www.elsevier.com/locate/jmrt

Original Article

Effect of the rheological properties of fresh binder on the compressive strength of pervious concrete

Sungwoo Park [a], Suhawn Ju [a], Hyeong-Ki Kim [b], Yo-Seob Seo [c], Sukhoon Pyo [a,*]

[a] Department of Urban and Environmental Engineering, Ulsan National Institute of Science and Technology (UNIST), 50 UNIST-gil, Ulju-gun, Ulsan, Republic of Korea

[b] Department of Architectural Engineering, Chosun University, 309 Pilmun-daero, Dong-gu, Gwangju, 61452, Republic of Korea

[c] Department of Oral and Maxillofacial Radiology, College of Dentistry, Chosun University, 309 Pilmun-daero, Dong-gu, Gwangju, 61452, Republic of Korea

ARTICLE INFO

Article history:
Received 25 October 2021
Accepted 8 January 2022
Available online 13 January 2022

Keywords:
Adhesion energy
CT scan
Flowability
Pervious concrete
Rheology

ABSTRACT

This paper investigates the effect of the rheological properties of fresh binder on the compressive strength of pervious concrete. Pervious concrete can be used to reduce stormwater runoff, urban heat island effect, or noise. Because of a limited amount of binder, the compressive strength of pervious concrete is one of the most critical properties for its structural applications. Although researchers have revealed the important factors contributing to the compressive strength of pervious concrete, still the effect of rheological properties of fresh binder have been rarely investigated. This study measured the plastic viscosity, yield stress, adhesion energy of fresh binder using a rotational rheometer; and the data were compared with the compressive strength of the pervious concrete. The experimental variables were flowability and water-to-cement (w/c) ratios of binder materials, target porosity, and the adoption of silica fume and fibers. The test results indicate that the adhesive energy results in the best correlation with compressive strength among various rheological properties. Three-dimensional computed tomography (CT) scanning test also demonstrates the effect of the rheological conditions of the binder on the homogeneity of pervious concrete.

1. Introduction

The porosity of pervious or porous concrete generally ranges between 15 and 35% [1–4]. This concrete has been widely studied because it helps in the reduction of stormwater runoff, urban heat island effect, and noise created through tire-pavement interaction. These effects largely depend on the amount of pores inside concrete and their connectivity. The more concrete contains pores inside, the more it becomes water-permeable, sound-absorbable, and low heat-capacity material. However, the pores in pervious concrete significantly reduce its compressive strength. Therefore, studies have been conducted to reveal the mix designs of pervious

* Corresponding author.
E-mail address: shpyo@unist.ac.kr (S. Pyo).

https://doi.org/10.1016/j.jmrt.2022.01.045

concrete which exhibit certain levels of compressive strength as well as other performances.

Many factors affect the quality of pervious concrete, such as type of aggregate, size of aggregate, supplementary cementitious materials, or fibers. Studies reported an appropriate range of aggregate size approximately 10–20 mm [1,5] including the effectiveness of blending different aggregate sizes [6]. Various types of aggregates were found to affect the compressive strength of pervious concrete [7–10]. Supplementary cementitious materials such as silica fume, ground granulated blast furnace slag, fly ash, or metakaolin improved concrete strength [2,11,12], especially, silica fume with superplasticizer was also effective to increase abrasion resistance [11]; Polymers improved compressive strength, permeability, and freez-thaw resistance of pervious concrete [13]; Fibers were able to create pores interconnected along the fibers and improved the tensile and flexural strength [14–16]; and Sun et al. [17] adopted alkali-activated geopolymer as binder of pervious concrete because of its higher viscosity than cementitious material.

Despite the extensive researches on pervious concrete, no study attributes the desirable rheological properties of fresh binder in pervious concrete. Since a minimal amount of binder is applied to pervious concrete, the effects of the characteristics of binder on the quality of pervious concrete can be critical. For example, the flowability of binder definitely affects the compressive strength and porosity of pervious concrete. If the flow of the binder is too low, pervious concrete does not mix homogeneously [9], whereas if the binder is too flowable segregation happens [18]. In both extreme conditions, flow-ability degrades the compressive strength of pervious concrete. Some studies suggested the desired binder flowability range of 150–230 mm [7,8,16]. However, this range was empirically determined based on the workability, and the effect of different flowability on compressive strength was not discussed. Kunhanandan Nambiar and Ramamurthy [19] advised appropriate spreadability and fluidity of pervious concrete using flow cone test (ASTM C939 [20]) and Marsh cone test, respectively. However, the study does not show the influence of binder flowability on the compressive strength and porosity of pervious concrete.

The main purpose of the current study is to reveal the rheological properties of the fresh binder with higher compressive strength of pervious concrete. It is hypothesized that the appropriate range of flowability can be different between binders of different mix designs. Furthermore, flowability alone may not be able to determine the suitability of binder mix design; perhaps other rheological properties such as viscosity, yield stress, and adhesiveness can be important factors because they are not always correlated to flowability [21]. By accompanying the compressive strength and the porosity measurements on pervious concrete, the desirable rheological conditions of the binder for pervious concrete are discussed. Three-dimensional (3D) computed tomography (CT) scan is incorporated to investigate pore distribution in the pervious concrete specimens. This paper is believed to show insights on the development of the binder mix design for pervious concrete in terms of compressive strength.

2. Materials and test methods

2.1. Raw materials

Slag cement was prepared by replacing 20% of cement with ground granulated blast-furnace slag (GGBS). Both the GGBS and cement type III were provided by Hanpil ENG., and their chemical compositions are shown in Table 1. Silica fume was MicroSilica PK940U from ELKEM and it contains amorphous SiO_2 of more than 95%. The particle size distributions of cement, slag, and silica fume are shown in Fig. 1. The mean particle size distributions of cement, slag, and silica fume are 7.35, 3.82, and 9.69 μm, respectively. Natural kenaf fibers of 10 mm length provided by Soo Industries Co., were also exploited to investigate their effect. The kenaf fibers consist of cellulose of 45–57 wt%, Hemicellulose of 22 wt%, Lignin of 8–13 wt%, and Pectin of 3–5 wt%; their tensile strength and Young's modulus are 930 MPa and 53 GPa, respectively; and the specific gravity is 1.9. A polycarboxylate-based superplasticizer was applied to adjust the flowability of the binder. The coarse aggregate was supplied from Hando Asphalt Co., and its sizes are in the range of 9–11 mm.

2.2. Mix design and specimen preparation

The brief design concept of pervious concrete is filling parts of the voids between aggregate with binder to achieve the target

Table 1 – Oxide percentage of cement and GGBS.

Constituent	Cement	GGBS
CaO	64.25	42.70
SiO_2	18.50	30.42
SO_3	4.56	3.15
Fe_2O_3	3.92	0.88
Al_2O_3	3.76	13.92
MgO	2.06	6.71
K_2O	1.42	0.65
Na_2O	0.02	0.28

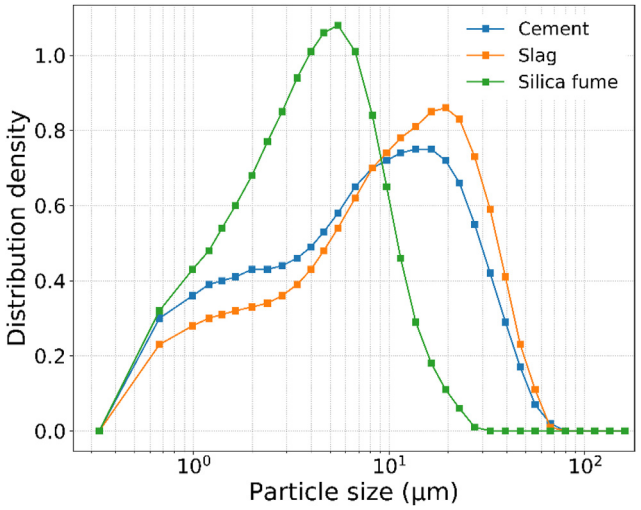

Fig. 1 – Particle size distribution of cement, slag, and silica fume.

porosity. Thus, the pervious concrete mix design should begin with measuring the bulk porosity of aggregate compacted. After filling a prism mold of size 300 × 300 × 150 mm with aggregate, it was compacted by rodding the surface until the aggregate surface did not sink anymore. The bulk density of aggregate (ρ_a) is calculated by dividing the weight of the aggregate by the volume of the mold. The bulk porosity of the aggregate (P_a) is, then, obtained by Eq. (1).

$$P_a = 1 - \frac{\rho_a}{\rho_w G_a} \times 100(\%) \quad (1)$$

where G_a and ρ_w are specific gravity of aggregate and density of water, respectively. It is noted that the target porosity of pervious concrete should be lower than P_a. The volume of the binder is obtained by subtracting the target porosity from P_a and multiplying to the entire volume of the specimen.

After the volume of the binder was calculated, binder was synthesized through the following steps: i) pour the solid powders into a mixing bowl and mix them for 5 min; ii) add water and superplasticizer into the mixture and further mix for another 10 min; and iii) for the specimens with fibers, add fibers gradually and mix for 5 min. After synthesizing binder, it is mixed with aggregate for more than 15 min until the mixture looks homogeneous.

The list of pervious concrete specimens is summarized in Table 2. To investigate the effect of binder material, five different mix designs were used for the pervious concrete of 15% target porosity. The 15% porosity was determined to observe the effect of flow and/or rheological properties of binder on the compressive strength of pervious concrete with a large amount of binder. Without silica fume, the w/c ratios of the binders were 0.25 and 0.30. With silica fume, the w/c ratio of the binders was fixed as 0.25 and the dosages of silica fume were 10% and 20% of cement weight. The natural fibers were added to the binder with 20% silica fume and its dosage was 2% of the cement paste volume in the pervious concrete. To investigate the effect of binder flowability on the compressive strength, the pervious concrete specimens with the target porosities of 15%, 20%, and 25% were prepared using the binder that contains 20% silica fume. For all specimens, three different flow levels of the binders were formulated using different amounts of superplasticizer; L, M, and H in Table 2 denote the low flow (170 mm), the medium flow (210 mm), and the high flow (250 mm), respectively. It is noted that the pervious concrete with fibers does not have the specimen of high flow because the amount of superplasticizer required is higher than the dosage limit suggested by the manufacture. The volume of the binder is calculated as the sum of the volumes of the ingredients using their specific gravity data as shown in Table 3. The specific gravities of cement, silica fume, aggregate, and fiber are 3.14, 2.2, 2.71, and, 1.9 respectively.

2.3. *Flowability, compressive strength, and porosity measurements*

The flow table test for the fresh binders was performed in accordance with ASTM C230 [22]. The amounts of superplasticizer for the targeted flows were determined through several trial tests. The compressive strength tests were conducted on both pervious concrete and hardened binder, in which 100 × 200 mm cylindrical molds and 50 × 50 × 50 mm cube molds were used for the concrete and the binder, respectively. Pervious concrete was cast in the cylindrical mold in two layers, and each layer was compacted by rodding the surface 90 times. The number of rodding was determined empirically until the surface did not sink. After one day of curing within the sealed mold, the specimens were removed from the molds and submerged in water until tested. The 28-day compressive strengths of pervious concrete and hardened binder were determined using ASTM C1231 [23] and ASTM C109 [24], respectively. For porosity measurement, the specimens were cast in the same cylindrical mold for compressive strength, cured for 3 days, and dried in the oven at 45 °C for 2 days. The volume of a specimen was measured following the method described in ASTM C127 [25], the pore volume is calculated by subtracting the volume of a cylindrical mold with the volume of a specimen, and the porosity was determined as the ratio of the pore volume to the volume of a cylindrical mold. The averages of three replicates were used as representative results for both porosity and compressive strength.

Table 2 – Mix designs of pervious concrete.

Specimen name	Target porosity (%vol.)[a]	Design parameter			Material weight (kg/m^3)					
		w/c ratio	SF[b] (%cw.)[c]	Fiber (%cv.)[d]	Aggregate	Cement	Water	SF	Fiber	SP (L,M,H)[e]
w/c 0.25	15	0.25	–	–	1546.2	482.0	120.5	–	–	(3.9, 6.3, 8.7)
w/c 0.30	15	0.30	–	–		443.1	132.9	–	–	(1.3, 3.5, 5.5)
w/c 0.25 – SF10	15	0.25	10	–		423.7	117.7	47.1	–	(8.0, 9.9, 11.8)
w/c 0.25 – SF20	15	0.25	20	–		368.0	115.0	92.0	–	(9.2, 11.0, 13.3)
w/c 0.25 – SF20F	15	0.25	20	2		360.6	112.7	90.2	9.8	(11.7, 20.3, -)
w/c 0.25 – SF20 (20%)	20	0.25	20	–		300.9	94.0	75.2	–	(7.5, 9.0, 10.9)
w/c 0.25 – SF20 (25%)	25	0.25	20	–		233.7	73.0	58.4	–	(5.8, 7.0, 8.5)

[a] Percentage to the total volume of pervious concrete.
[b] Silica fume.
[c] Percentage to cement weight.
[d] Percentage to cement paste volume.
[e] Amounts of superplasticizer for targeted flows of fresh binders. L: low flow (170 mm), M: medium flow (210 mm), H: high flow (250 mm).

Table 3 – The volume of fresh binder of pervious concrete.

Specimen name	Volume (m^3)					
	Target void	Binder	Cement[a]	Water	SF[b]	Fiber[c]
w/c 0.25	0.150	0.274	0.154	0.120	–	–
w/c 0.30	0.150	0.274	0.141	0.133	–	–
w/c 0.25 – SF10	0.150	0.274	0.135	0.118	0.021	–
w/c 0.25 – SF20	0.150	0.274	0.117	0.115	0.042	–
w/c 0.25 – SF20F	0.150	0.274	0.115	0.113	0.041	0.005
w/c 0.25 – SF20 (20%)	0.200	0.224	0.096	0.094	0.034	–
w/c 0.25 – SF20 (25%)	0.250	0.174	0.074	0.073	0.027	–

The aggregate volume = 1546.17 (kg)/2.71/1000 = 0.576 m^3.
The binder volume = 1–0.576-target void.
[a] Cement weight (kg)/3.14/1000.
[b] Silica fume weight (kg)/2.2/1000.
[c] Fiber weight (kg)/1.96/1000.

2.4. *Rheological properties measurements*

A rotational rheometer (HAAKE MARS III, Thermo Fisher Scientific Inc.) with parallel plates was used to measure the rheological properties of fresh binder. After mixing, fresh binder was placed on the lower plate, and the upper plate was lowered until the gap between the upper plate and the lower plate became 2 mm. The upper plate was run by the test procedure in Fig. 2. The binder rested between the plates for 25 s and the shear rate of the upper plate increased linearly up to 70 s^{-1} and maintained for 80 s. After the pre-shear, the shear stress was measured with the step-wised reduction of shear rate and each step ran for 15 s. The average values of the shear stress at the steps of the shear rate from 10 to 70 s^{-1} were applied to a Bingham model to calculate plastic viscosity and shear yield stress [26–30]; the plastic viscosity and the yield stress are the tangent and the intercept of the linear regression, respectively. It should be noted that the sandpapers of 120 grits were attached to the surfaces of the upper and lower plates to prevent the slip between the plates and the binder [28].

After the rotational rheology test, the fresh binder rested for 30 s and the adhesion test was carried out. The upper plate moved upward with the speed of 0.028 mm/s, and the adhesive force and displacement of the upper plate were measured [28]. Fig. 3 shows an example of the adhesion test results of the specimens of w/c 0.25 – SF20. The data of the maximum adhesive forces and the adhesion energies that the area under the curve up to 5 mm displacement are discussed in this paper.

2.5. *3D CT scanning measuremen*

The porosity of hardened specimens was also measured via 3D CT scanning. Cone-beam computed tomography with a voxel size of 0.3 mm was used and the detection conditions were a voltage of 100 kVp and a current of 30 mA. The porosity was calculated by counting the pixels of the darker and brighter portions, which indicates pores and skeletons, respectively. The cross-sectional CT images in Fig. 4 were filtered using the 2-D adaptive noise-removal filter (Wiener filter) available in the Matlab™ software. The region of interest (ROI) for this filtering was fixed as 10 cm diameter, i.e., the diameter of concrete specimens. The gray-level histogram gave distinctive regions allowing the determination of

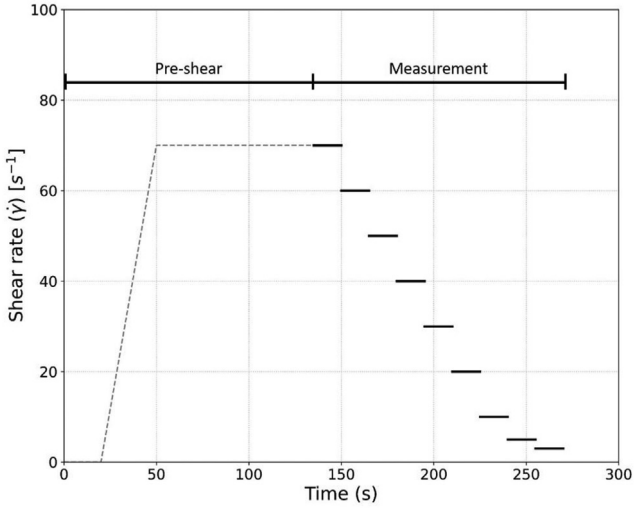

Fig. 2 – The rheology test procedure.

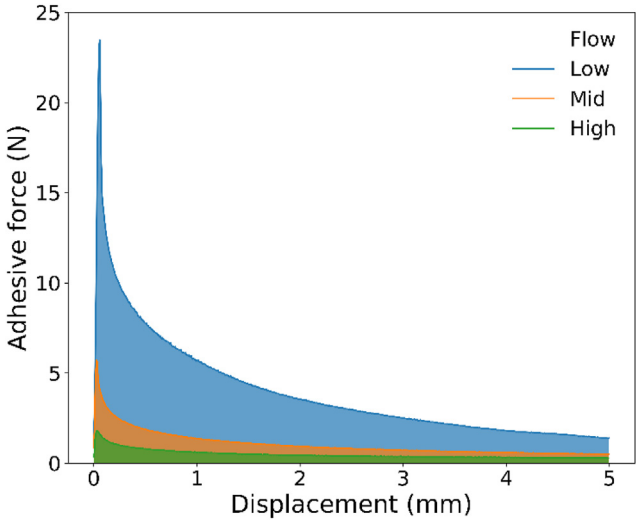

Fig. 3 – An example of rheology test results of w/c 0.25 - SF20 specimens.

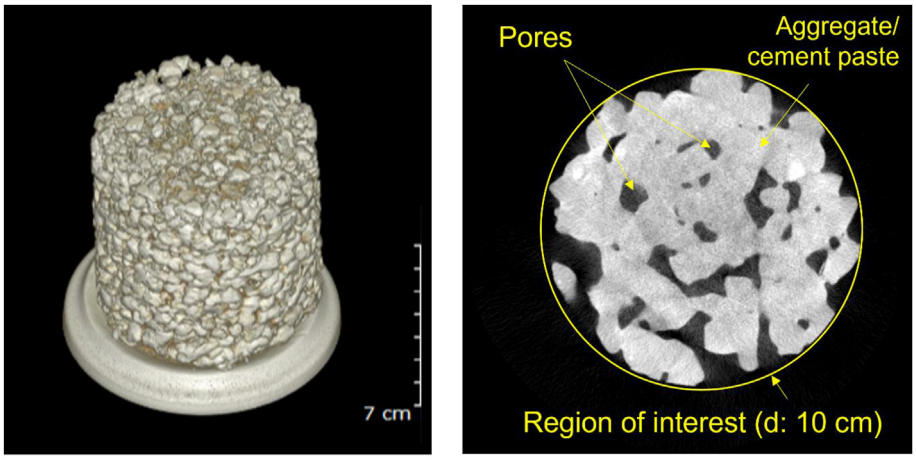

Fig. 4 – An example of CT scan results of porous concrete: (a) compiled 3D image, and (b) cross-sectional image.

thresholds for quantifying the areas corresponding to skeletons and pores. Based on this, the porosity profile of the specimens by height was obtained.

3. Results and discussions

3.1. *Compressive strength and porosity of pervious concrete*

The 28-day compressive strength and the porosity data of the pervious concrete specimens with different binder mixtures are shown in Fig. 5. It should be noted that the specimens used for porosity measurements are different from those used for the compressive strength, and, therefore, the actual porosity and the compressive strength may not be matched perfectly. However, since the standard deviation values of porosity data are less than 2%, and the specimens used for compressive strength can be assumed to have a similar porosity. Some of the specimens result in higher errors such as w/c 0.25 - SF10 (M), w/c 0.25 – SF20 (L), and w/c 0.25 – SF20F (L), which can be attributed to the unstable structure of pervious concrete. Nevertheless, the consistency among the specimens in each group can be inferred by the low errors in the porosities. The pervious concrete specimens result in different compressive strength values with different flows of fresh binders even if the same recipe was used except the amount of superplasticizer. The effect of the amount of superplasticizer on the compressive strength of the hardened binder is negligible, as shown in Table 4. The previous study reported the same results [31]. Some of the specimens of the low flow exhibit distinctively lower compressive strength. It can be assumed that the specimens have macro-sized pores caused by the low flow level.

The differences in the compressive strength of pervious concrete can be attributed to other reasons, such as the segregation of binder. The high flow leads to the lowest compressive strength for all specimens, which is because of the segregation of the binder. For example, Fig. 6 shows the pictures of the specimens of w/c 0.25 - SF20 with different flows. As the flow increases, the surface of pervious concrete becomes smoother by being filled with a more amount of binder. Especially, in the case of the high flow, the paste has flown down to the bottom, which is evidence of segregation.

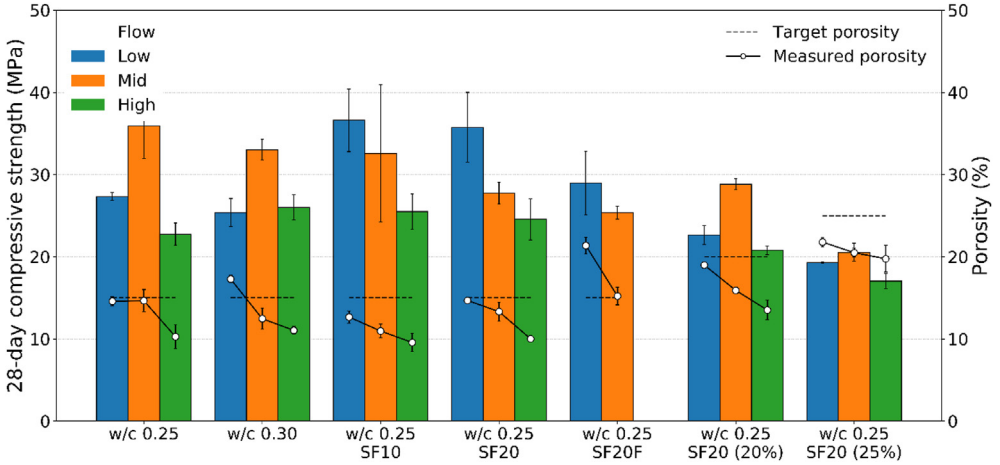

Fig. 5 – 28-day compressive strength of pervious concrete specimens with different flows of fresh binders.

Table 4 – The 28-day compressive strength of the hardened binders.

Specimen	28-day compressive strength (MPa) (COV (%))[a]		
	Flow L	Flow M	Flow H
w/c 0.25	79.5 (17.8)	116.7 (11.6)	123.9 (6.7)
w/c 0.30	103.2 (2.4)	100.5 (11.9)	105.2 (4.9)
w/c 0.25 – SF10	119.1 (27.1)	114.8 (2.2)	123.3 (13.7)
w/c 0.25 – SF20	96.0 (16.4)	111.7 (15.0)	109.8 (23.8)
w/c 0.25 – SF20F	93.7 (2.1)	95.4 (3.5)	–

[a] Coefficient of variation of the compressive strength.

Since the amount of superplasticizer does not affect the compressive strength of fresh binder, it can be concluded that the flow itself affects the compressive strength of pervious concrete.

However, the flow of fresh binder cannot explain the compressive strength of the specimens of the medium flow and the low flow. The flow of the highest compressive strength of pervious concrete is different with a different binder mixture even when the target porosity is the same. For example, in the case of the pervious concrete of w/c 0.25 and w/c 0.30, the highest compressive strength values are achieved by the medium flow. On the other hand, the pervious concrete with silica fume in binder such as the specimens of w/c 0.25 – SF10, w/c 0.25 - SF20, and w/c 0.25 - SF20F attain the highest compressive strength with the low flow. Furthermore, the flow of the highest compressive strength of pervious concrete is different with a different target porosity even when the mixture of the binder is the same; for example, in the case of the pervious concrete of w/c 0.25 - SF20, the highest compressive strengths are achieved by the low and the medium flows when the target porosities are 15% and 20%, respectively. This implies that other rheological properties such as plastic viscosity, yield stress, or adhesive characteristics, possibly are important factors for the compressive strength of pervious concrete.

The 28-day compressive strength and the porosity data of the pervious concrete specimens with different target porosities are also shown in Fig. 5; the specimens of w/c 0.25 - SF20 with the porosities of 15%, 20%, and 25%. The compressive strength decreases with the increase of the target porosity. The effect of the flow on the compressive strength of pervious concrete also declines when the target porosity increases because the amount of fresh binder is smaller. For example, the difference between the maximum and minimum averaged compressive strengths of the specimens of the target porosity of 25% is only 3.5 MPa, whereas the difference of the specimens of 15% is 11.2 MPa. This may indicate that the effect of the rheological properties of the fresh binder on the compressive strength of pervious concrete is more significant when the target porosity is lower. It is also noted that the flow that results in higher compressive strength of pervious concrete is changed from the low to the medium when the target porosity increases from 15% to 20%. This can be inferred that when the amount of the binder is lower, the higher flow of the fresh binder can be advantageous because the binder needs to be spread wider to fill the voids equally. Therefore, the appropriate rheological properties of the fresh binder can be also dependent on the amount of the binder required in pervious concrete.

In this study, the usage of the natural fibers degrades the compressive strengths in both paste and concrete. It has been reported that fibers can improve the durability of pervious concrete [32]. However, it is not clear that fibers are beneficial in terms of the compressive strength. It can be assumed that the amount of the binders and the fibers are too little to tangle with aggregates, and, therefore, they cannot enhance the mechanical property of pervious concrete.

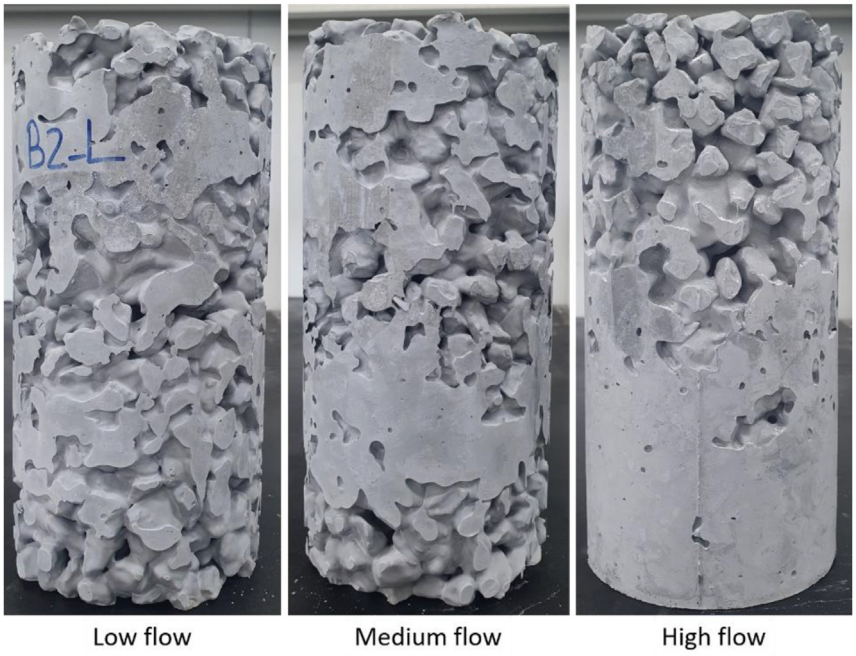

Fig. 6 – The pervious concrete specimens of w/c 0.25 - SF20 with different flows.

An interesting trend is observed from Fig. 7 showing the relationship between the porosity and the compressive strength. In the plot, no clear correlation is observed and the specimens of the same target porosity of 15% do not present the typical relationship between the porosity and the compressive strength. It is generally known that the compressive strength of pervious concrete decreases with the increase of the porosity [29,33–35]. The data of the high flow in green markers result in lower porosities of pervious concrete, however, their compressive strengths are similar to or lower than those of the low and the medium flows because of the segregation as aforementioned. In consequence, the compressive strength of pervious concrete does not always have a good correlation with the porosity when it is determined by the flow of fresh binder, not by the target porosity.

The relationship between the porosity and the compressive strength of the pervious concrete with a different target porosity is shown in Fig. 8. In this plot, the typical trend of the relationship can be observed; the compressive strength decreases with the increase of porosity. This trend becomes clearer when the data of the specimens with the same flow are compared. The compressive strength of pervious concrete exhibits a well-known correlation of decline with the increase of the porosity when the flow of fresh binder remains the same and the target porosity is different. In other words, the flow of fresh binder affects the compressive strength of pervious concrete as well as the porosity.

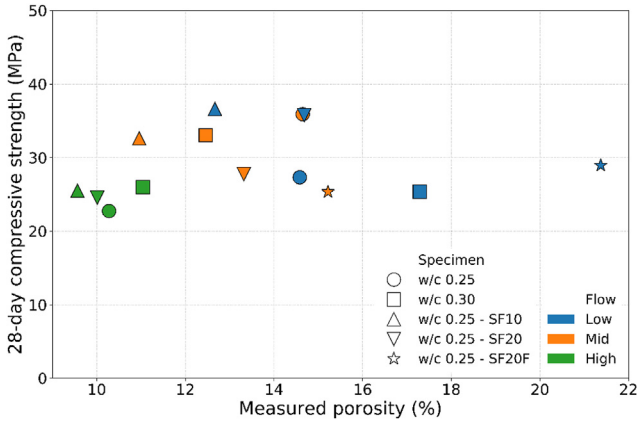

Fig. 7 – The relationship between the 28-day compressive strength and the porosity of the pervious concrete specimens with different binders (target porosity: 15%).

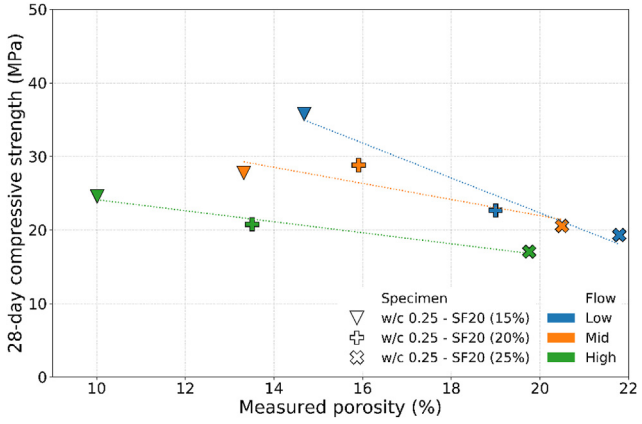

Fig. 8 – The relationship between the 28-day compressive strength and the porosity of the pervious concrete specimens with different target porosities.

3.2. *Rheology*

3.2.1. *Viscosity and yield stress*

Fig. 9 shows the results of the rheology tests on the fresh binders. The X-axis is the shear rate and the Y-axis is the shear stress. The data show almost parallel linear regressions and they are shifted down as the flow increases except for the w/c 0.25 specimen. The data lines of the specimen without silica fume are shifted down significantly from flow M, while the data of the specimens with silica fume are shifted down significantly from L. This can be because of the synergistic effect of silica fume and polycarboxylate-based superplasticizer on the flow of fresh binder; silica fume helps the dispersion of particles along with polycarboxylate-based superplasticizer [36]. The w/c 0.25 specimen shows a different tendency of the results; the tangents of the linear regressions increase significantly when the flows increase from low to medium, and, then, the lines are shifted down almost parallelly when the flows increase from medium to high. It should be pointed out that the different tendency is because of the slip between the rheometer plates and the specimens. The fresh binder of the w/c 0.25 (L) strongly agglomerates and is not broken easily, and their surface was drier compared to other fresh binders. Although the sandpapers were applied to prevent the slip, the friction force seemed not sufficient.

Based on the Bingham model, the tangent of the linear regression data is the plastic viscosity and the intercept is the shear yield stress. The plastic viscosity indicates the resistance against flowing, and the shear yield stress means the minimum stress to cause the flow in static status [37]. The data of plastic viscosity and yield stress of the specimens are summarized in Fig. 10.

In the case of the binders without silica fume, the plastic viscosity decreases as the w/c ratio increases. It can be associated with that the number of unreacted cement particles decreases with a larger amount of mixing water. The plastic viscosity is different with a different flow level, which implies that the amount of the superplasticizer affects the viscous interaction between cement particles. In the case of the binders with silica fume, the level of plastic viscosity decreases with the increase of silica fume dosage, which can be attributed to the smooth surface of silica fume and its interaction with the polycarboxylate-based superplasticizer [38]. The plastic viscosities of the w/c 0.25 – SF10 and SF20 do not change along with the flow of the fresh binder, which is different from the specimens without silica fume. The yield stress is higher with a lower flow for all cases. It is also noted that silica fume increases the yield stress of the fresh binder with the same w/c ratio of 0.25 [38]. The higher yield stress can be associated with unreacted particles because of the lower water content or because of the additional silica fume particles. In summary, the specimens without silica fume exhibit

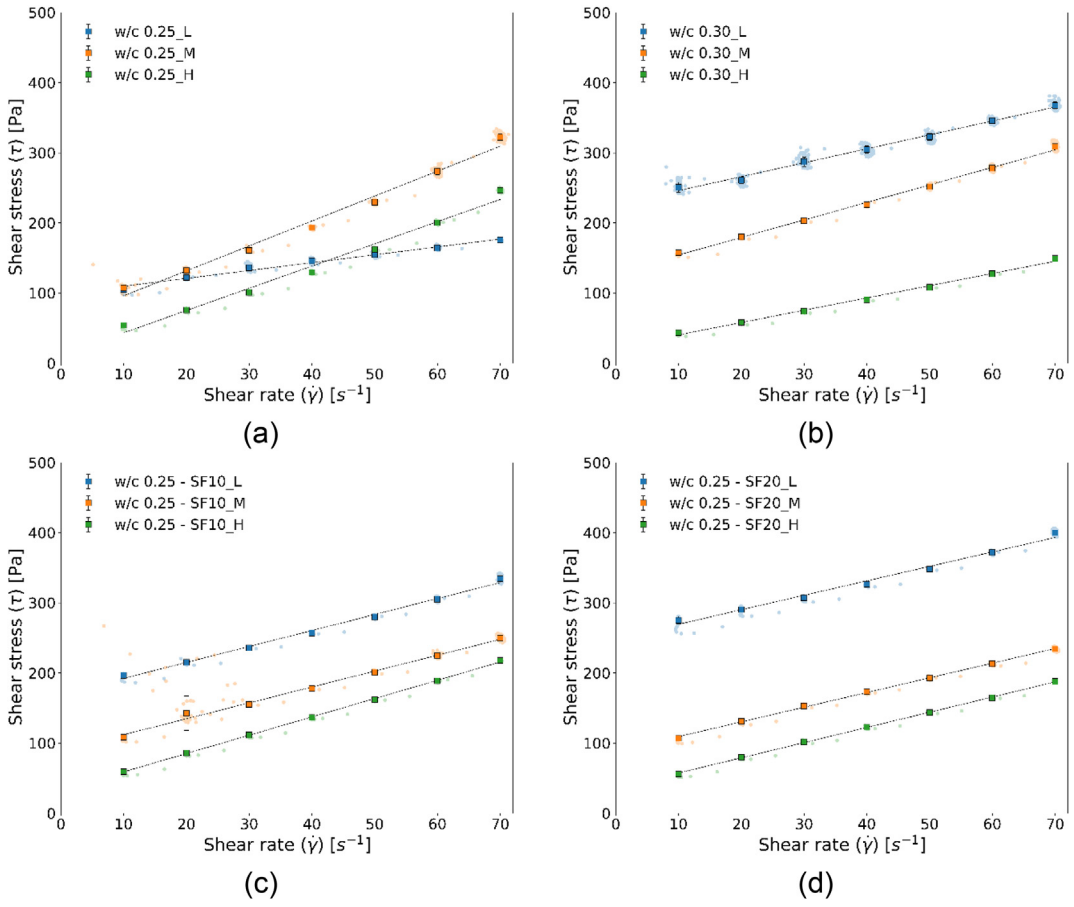

Fig. 9 – The rheology test results of fresh binders: (a) w/c 0.25, (b) w/c 3.0, (c) w/c 0.25 - SF10, and (d) w/c 0.25 - SF20.

the highest compressive strength with the highest plastic viscosity, and the specimens with silica fume exhibit the highest compressive strength with the highest yield stress. The combined effect of the plastic viscosity and the yield stress may affect the compressive strength, however, further study is required to reveal the accurate relationships.

3.2.2. *Adhesion*

Fig. 11 shows the adhesion test results. The peak of adhesive force decreases as the flow of fresh binder increases. The peak value appears in the initial movement of the plate, which can be considered as a static force. Therefore, the trend of the peak of adhesive force is the same as the shear yield stress in Fig. 10b, which does not coincide with the compressive strength data of pervious concrete in Fig. 5.

The adhesive energy shows a different tendency from the peak of adhesive force. The binders without and with silica fume exhibit the highest adhesive energy with the medium flow and the low flow, respectively. The different tendency of adhesive energy from the peak of adhesive force is attributed to the additional resistance of the fresh binder against segregation after it reaches the maximum adhesive force. The

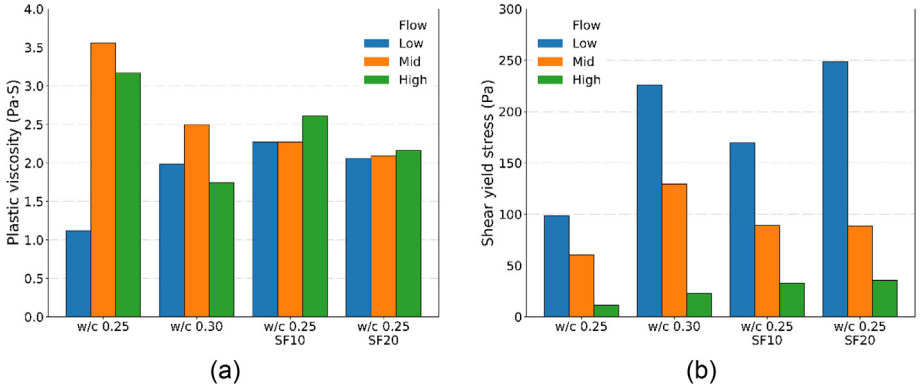

Fig. 10 – The rheology test results of fresh binders: (a) plastic viscosity and (b) yield stress.

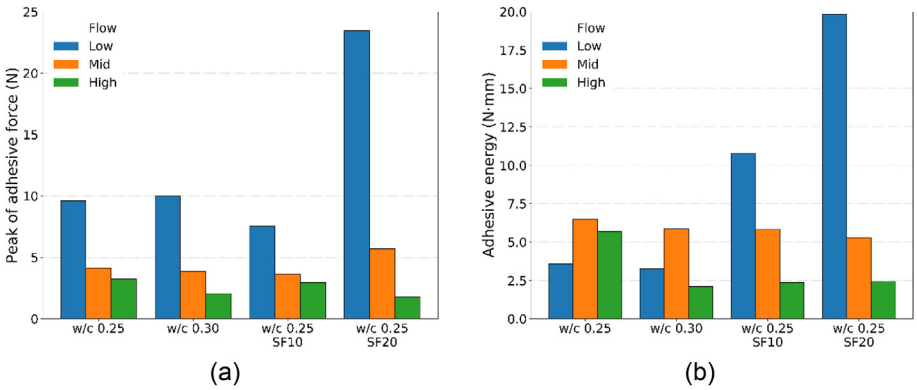

Fig. 11 – The adhesion test results of fresh binders: (a) peak of adhesive force and (b) adhesive energy.

additional resistant energy can be related to the plastic viscosity of dynamic status. For example, the specimens of w/c 0.25 and 0.30 have the highest peaks of adhesive force with the low flow while they exhibit the highest adhesive energies with the medium flow as they have the highest plastic viscosity with the medium flow. That is, plastic viscosity may affect the adhesive energy. Therefore, it can be concluded that the adhesive energy can represent the combined effect of plastic viscosity and yield stress of the fresh binder.

It should be noted that the medium flow is more favorable to the pervious concrete with the 20% silica fume when the target porosity is in the range of 20–25%. The reason is assumed that a smaller amount of fresh binder requires a lower adhesion energy as it needs to be spread wider for a homogeneous structure.

3.2.3. *Relationships between the compressive strength of pervious concrete and the rheological properties of fresh binder*

Fig. 12 shows the summary of the relationships between the 28-day compressive strength of pervious concrete and the rheological properties of fresh binder. Data are grouped by the specimens and the R-squared values of linear regressions are shown next to the specimen names.

Plastic viscosity in Fig. 12a does not show a correlation with the compressive strength. Although the correlation coefficients of the linear regression are higher than 0.80 except for the w/c 0.25 (L), the tendencies between the specimens with and without silica fume are different. This implies that the flowing resistance in dynamic status is a more critical factor to the mixing process than the compressive strength of pervious concrete. The shear yield stress in Fig. 12b shows a stronger relationship with the compressive strength of pervious concrete. The reason is assumed to be that the yield stress is more related to the casting and compacting process that can affect the homogeneity of pervious concrete as the yield stress means the flowing resistance in static status. That is, yield stress affects the quality of pervious concrete more significantly than plastic viscosity.

Adhesive energy in Fig. 12c has a linear relationship with the compressive strength of pervious concrete resulting in the correlation coefficients of the linear regression larger than 0.93 except for the w/c 0.25 specimen. While plastic viscosity and shear yield stress are the properties of the material itself, adhesive energy entails the feature of the interaction between the material and the object attached. In pervious concrete, fresh binder is the material and coarse aggregate is the object. Therefore, adhesive energy can be more related to the homogeneity of pervious concrete than plastic viscosity and shear yield stress. As a result, it can be concluded that the adhesive energy represents the resistance of the fresh binder against segregation caused by casting and compacting.

The reason for a weak linear relationship between the adhesive energy and the compressive strength of w/c 0.25 can be attributed to the data point of flow L. As aforementioned, the fresh binder of the w/c 0.25 (L) specimen has a strong agglomeration force and dry surface, and, thus, does not adhere to an object before it is hardened. Because of this peculiar characteristic, the rheology tests conducted in this study may not be suitable for the w/c 0.25 (L) specimen. However, it should be also noted that the workability of the w/c 0.25 (L) specimen is so poor that it seems not to be affordable for pervious concrete on a large scale. Even though other specimens with silica fume or of w/c 0.30 have the same flow of 150 mm, their workability is more adequate than w/c 0.25 (L), probably because of the lower plastic viscosity. In consequence, adhesive energy is still believed to represent the proper rheological properties of the fresh binder for pervious concrete with practical workability.

3.3. *CT scannning image*

To investigate the effect of the rheological properties of the fresh binder on the homogeneity of pervious concrete, the CT scan test was performed and the data are shown in Fig. 13. In each plot, X-axis is the porosity and Y-axis is the vertical location of the specimen in a cylindrical shape. The solid and the dashed lines are the average porosity of the CT scanning data and the target porosity of the specimen, respectively. In the case of the high flow, the porosity is very low as almost zero below half of the vertical level, which indicates the fresh binder sinks down to the bottom while casting and compacting. In the case of the medium and the low flows, the porosity lines can be divided into two parts that indicate the casting layers. In each layer, the porosity of the top is low and it increases almost linearly as the vertical level goes down. This implies that the fresh binders of the medium and the low flows can be held between aggregate during casting.

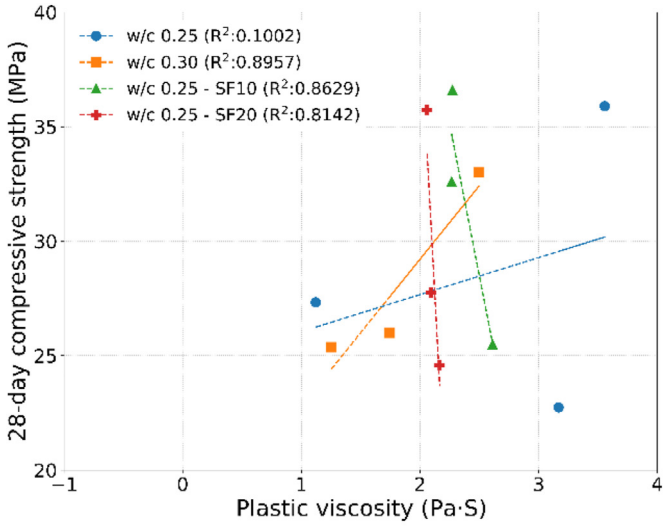

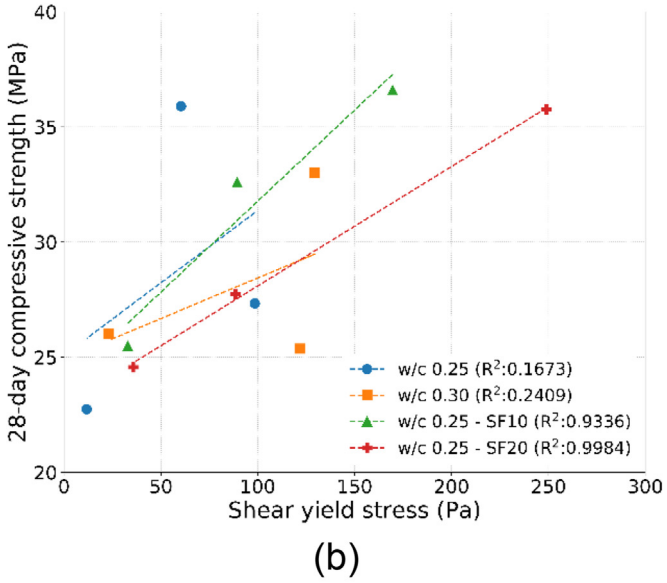

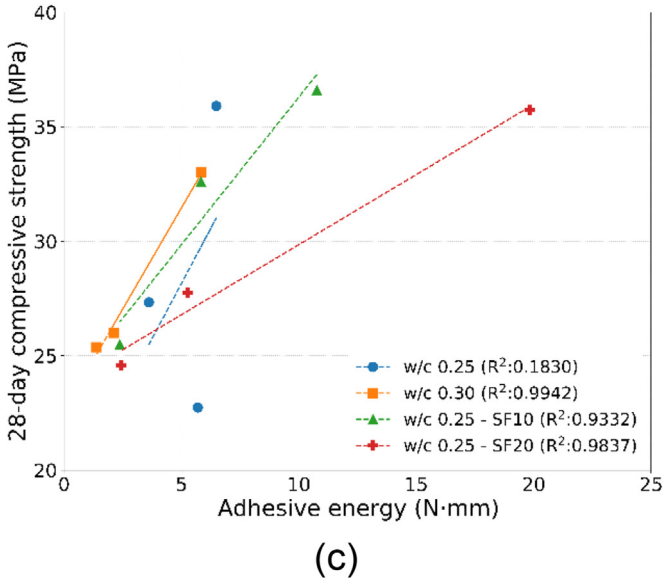

Fig. 12 – The relationships between the 28-day compressive strength of pervious concrete and the rheological properties of fresh binder: (a) plastic viscosity, (b) shear yield stress, (c) adhesive energy.

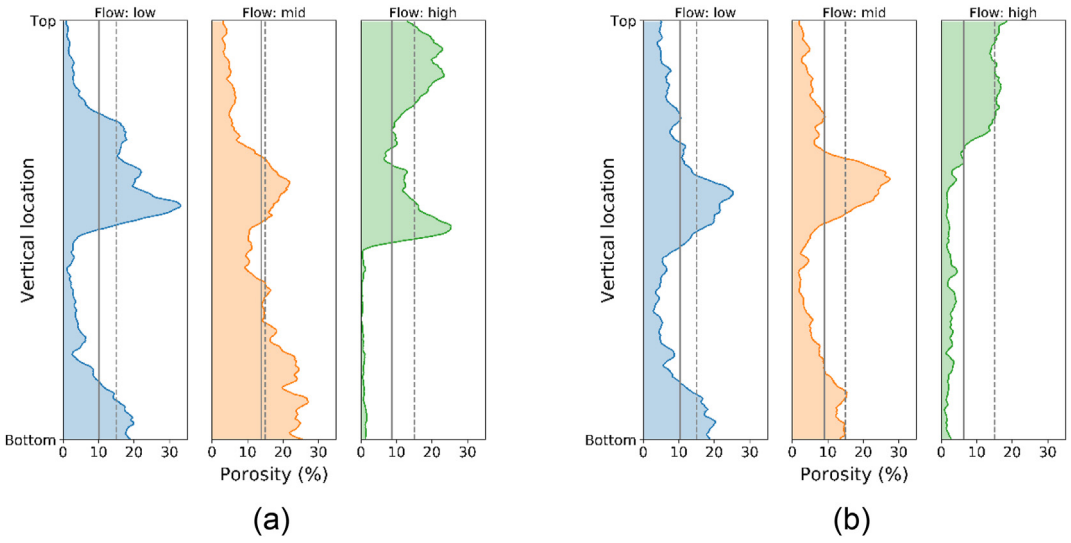

Fig. 13 – The porosity data from CT scan images of the pervious concrete specimens: (a) w/c 0.25 and (b) w/c 0.25 - SF20. The solid and the dashed lines are the average porosity of CT data and the target porosity, respectively.

The weak point of the pervious concrete is the middle where the porosity of the layer drastically spikes. Without silica fume, the specimen of w/c 0.25 in Fig. 13a, the porosity at the middle is higher with the low flow. This can be attributed to a higher force of agglomeration of fresh binder although its adhesion energy is lower than that of the medium flow. The fresh binder and aggregate are not mixed well, aggregate drops faster than the fresh binder, and the fresh binder remains only in the upper part of each casting layer resulting in the sharp increase of the porosity with the decrease of the vertical level. As a result, the porosity of the specimen of the medium flow is more constant than that of the low flow. With silica fume, the specimen of w/c 0.25 – SF20 in Fig. 13b, the specimen of the low flow has similar plot lines in the upper and lower layers. The specimen of the medium flow exhibits a larger amount of cement paste in the lower layer, which means the fresh binder sinks down more than that of the low flow resulting in the lower compressive strength. Therefore, it can be concluded that the fresh binder of the low flow has a higher resistance against sinking.

The porosity data obtained from the water absorption test and CT scan test were summarized in Table 5. The porosity values from the CT scan test were lower than those from the water absorption test. This might be because of the post-processing of CT scan test. The pore area in each image was calculated based on the color of the pixels; black area is considered as pores and bright area is considered as structure. However, in some pixels, the pixel color is gray because of the aggregate in a lower level and considered as structure. Since which of the porosities obtained from water absorption test or CT scan test is more correct value is out of scope in this paper, the distribution of porosity along with the specimen height is mainly discussed. The specimens of w/c 0.25 and w/c 0.25 – SF20 have the lowest coefficient of variation values with the medium flow and the low flow, respectively. This implies that those specimens have more homogeneous structures than others resulting in higher compressive strengths.

Table 5 – The results of porosity measurement of the pervious concrete specimens of w/c 0.25 and w/c 0.25 - SF20 (target porosity: 15%).

Specimen	Flow	Porosity measurement		
		Water absorption	CT scan	
		Porosity (%)	Porosity (%)	COV[a]
w/c 0.25	L	14.58	10.08	0.82
	M	14.65	13.88	0.51
	H	10.28	8.70	0.96
w/c 0.25 – SF20	L	14.68	10.40	0.57
	M	13.32	9.04	0.72
	H	10.01	6.30	0.91

[a] Coefficient of variation of the CT scan data along with the height of the specimen.

4. Summary and conclusions

This paper investigated the effect of the rheological properties of fresh binder on the compressive strength of pervious concrete. It was hypothesized that the appropriate flow value of fresh binder can be different with a different binder material, and, therefore, the flow, plastic viscosity, yield stress, and adhesion tests were performed on the various binders and those data were compared with the compressive strength of the pervious concrete made of the same binders. To demonstrate how the rheological properties affect the homogeneity of pervious concrete structure, the CT scan test was also conducted. The key findings and observations can be summarized as below:

1. Among the rheological properties of fresh binders, the adhesion energy has a linear correlation with the compressive strength of pervious concrete resulting in the correlation coefficients higher than 0.90; the higher the adhesion energy of the fresh binder, the greater the

compressive strength of the pervious concrete. This correlation can be found in both cement pastes without and with silica fume. Therefore, if a fresh binder is developed for the binder of pervious concrete, the adhesion test needs to be accompanied by the flow test.

2. The flow of fresh binder affects the porosity of pervious concrete; the porosity of pervious concrete decreases by around 5% as the flow increases from 150 to 250 mm even with the same target porosity because of the segregation of binder. However, the compressive strength of pervious concrete does not have any correlation with the porosity affected by the flow.
3. The compressive strength of pervious concrete has a clear correlation with the porosity when the flow is the same and the target porosity is different. However, the changes in the flow and the adhesion energy of the fresh binder can also affect the compressive strength of pervious concrete. The differences in the compressive strength of pervious concrete with different flow levels are around 25–30%. The natural fibers were observed to degrade the compressive strength of pervious concrete by 10% or higher, and, therefore, the effect of fibers needs to be investigated before their application.
4. From the CT scan test, it was observed that the rheological properties of fresh binder can affect the homogeneity of pervious concrete. When the adhesion energy of fresh binder increases from the lowest level to the highest level, the coefficient of variation of the porosity values of the layers along with the vertical level of pervious concrete decreases by around 50%, which means that the structure of pervious concrete is more homogeneous resulting in a higher compressive strength of pervious concrete.

Based on the findings, this paper suggests the measurement of adhesion energy of fresh binders to have a more homogeneous structure of the pervious concrete. The concept of the adhesion energy of fresh binder may be able to explain why the aggregate in a smaller size results in lower compressive strength of pervious concrete [1]. The adhesion energy of fresh binder can be generated with other objects attached, in the case of pervious concrete, to aggregates. Therefore, a larger surface area or smaller spacing of the smaller size aggregate requires a lower adhesion energy for the fresh binder to be spread well creating a more homogeneous structure of pervious concrete. If the appropriate adhesion energy in pervious concrete can be calculated concerning the size and the volume of aggregate, a more generalized design guideline of pervious concrete can be established in the function of the adhesion energy of fresh binders, the size and the volume of aggregate, design porosity, and the compacting method. In addition, the environmental and economical assessment on pervious concrete needs to be invested [39].

Declaration of Competing Interest

The authors declare that they have no conflicts of interests.

Acknowledgment

This work was supported by the National Research Foundation of Korea (NRF) grant funded by the Korea government (MSIT) (No. 2021R1C1C1008671). This study was also supported by the CNI Research Project Fund (1.210109.01) of UNIST (Ulsan National Institute of Science and Technology). The opinions expressed in this paper are those of the authors and do not necessarily reflect the views of the sponsors.

REFERENCES

[1] Yu F, Sun D, Wang J, Hu M. Influence of aggregate size on compressive strength of pervious concrete. Construct Build Mater 2019;209:463–75. https://doi.org/10.1016/j.conbuildmat.2019.03.140.
[2] Saboo N, Shivhare S, Kori KK, Chandrappa AK. Effect of fly ash and metakaolin on pervious concrete properties. Construct Build Mater 2019;223:322–8. https://doi.org/10.1016/j.conbuildmat.2019.06.185.
[3] Chen X, Shi D, Shen N, Li S, Liu S. Experimental study and analytical modeling on fatigue properties of pervious concrete made with natural and recycled aggregates. Int J Concr Struct Mater 2019;13:10. https://doi.org/10.1186/s40069-018-0305-0.
[4] Liu R, Chi Y, Chen S, Jiang Q, Meng X, Wu K, et al. Influence of pore structure characteristics on the mechanical and durability behavior of pervious concrete material based on image analysis. Int J Concr Struct Mater 2020;14:29. https://doi.org/10.1186/s40069-020-00404-1.
[5] Kim JH, Mondal P, Shah SP. Cement-based materials characterization at nanoscale: nanoindentation and ultrasonic atomic force microscopy (AFM). Am Concr Institute, ACI Spec Publ; 2010.
[6] Marolf A, Neithalath N, Sell E, Wegner K, Weiss J, Olek J. Influence of aggregate size and gradation on acoustic absorption of enhanced porosity concrete. ACI Mater J 2004;101:82–91. https://doi.org/10.14359/12991.
[7] Park SB, Seo DS, Lee J. Studies on the sound absorption characteristics of porous concrete based on the content of recycled aggregate and target void ratio. Cement Concr Res 2005;35:1846–54. https://doi.org/10.1016/j.cemconres.2004.12.009.
[8] Ngohpok C, Sata V, Satiennam T, Klungboonkrong P, Chindaprasirt P. Mechanical properties, thermal conductivity, and sound absorption of pervious concrete containing recycled concrete and bottom ash aggregates. KSCE J Civ Eng 2018;22:1369–76. https://doi.org/10.1007/s12205-017-0144-6.
[9] Kim HK, Lee HK. Influence of cement flow and aggregate type on the mechanical and acoustic characteristics of porous concrete. Appl Acoust 2010;71:607–15. https://doi.org/10.1016/j.apacoust.2010.02.001.
[10] Xiao J, Ma Z, Sui T, Akbarnezhad A, Duan Z. Mechanical properties of concrete mixed with recycled powder produced from construction and demolition waste. J Clean Prod 2018;188:720–31. https://doi.org/10.1016/j.jclepro.2018.03.277.
[11] Yang J, Jiang G. Experimental study on properties of pervious concrete pavement materials. Cement Concr Res 2003;33:381–6. https://doi.org/10.1016/S0008-8846(02)00966-3.
[12] Pachideh G, Gholhaki M, Moshtagh A. Experimental study on mechanical strength of porous concrete pavement

containing pozzolans. Adv Civ Eng Mater 2020;9:20180111. https://doi.org/10.1520/ACEM20180111.
[13] Kevern JT. Advancements in pervious concrete technology. Iowa State University; 2008.
[14] Falliano D, De Domenico D, Ricciardi G, Gugliandolo E. Compressive and flexural strength of fiber-reinforced foamed concrete: effect of fiber content, curing conditions and dry density. Construct Build Mater 2019;198:479–93. https://doi.org/10.1016/j.conbuildmat.2018.11.197.
[15] Khan M, Ali M. Effect of super plasticizer on the properties of medium strength concrete prepared with coconut fiber. Construct Build Mater 2018;182:703–15. https://doi.org/10.1016/j.conbuildmat.2018.06.150.
[16] Yoon J, Kim H, Koh T, Pyo S. Microstructural characteristics of sound absorbable porous cement-based materials by incorporating natural fibers and aluminum powder. Construct Build Mater 2020;243:118167. https://doi.org/10.1016/j.conbuildmat.2020.118167.
[17] Sun Z, Lin X, Vollpracht A. Pervious concrete made of alkali activated slag and geopolymers. Construct Build Mater 2018;189:797–803. https://doi.org/10.1016/j.conbuildmat.2018.09.067.
[18] Valore RC, others. Insulating concretes. J. Proc. 1956;53:509–32.
[19] Kunhanandan Nambiar EK, Ramamurthy K. Fresh state characteristics of foam concrete. J Mater Civ Eng 2008;20:111–7. https://doi.org/10.1061/(ASCE)0899-1561(2008)20:2(111).
[20] Standard test method for flow of grout for preplaced-aggregate concrete (flow cone method). West Conshohocken, PA, https://doi.org/10.1520/C0939_C0939M-16A; 2017.
[21] Banfill PFG. Rheology of fresh cement and concrete. Abingdon, UK: Taylor & Francis; 1991. https://doi.org/10.4324/9780203473290.
[22] Standard specification for flow table for use in tests of hydraulic cement. West Conshohocken, PA. 2021. https://doi.org/10.1520/C0230_C0230M-21.
[23] Standard practice for use of unbonded caps in determination of compressive strength of hardened cylindrical concrete specimens. West Conshohocken, PA. 2016. https://doi.org/10.1520/C1231_C1231M-15.
[24] Standard test method for compressive strength of hydraulic cement mortars (using 2-in. Or [50-mm] cube specimens). West Conshohocken, PA. 2016. https://doi.org/10.1520/C0109_C0109M-16A.
[25] Standard test method for relative density (specific gravity) and absorption of coarse aggregate. West Conshohocken, PA. 2015. https://doi.org/10.1520/C0127-15.
[26] Gołaszewski J, Szwabowski J. Influence of superplasticizers on rheological behaviour of fresh cement mortars. Cement Concr Res 2004;34:235–48. https://doi.org/10.1016/j.cemconres.2003.07.002.
[27] Ting L, Qiang W, Shiyu Z. Effects of ultra-fine ground granulated blast-furnace slag on initial setting time, fluidity and rheological properties of cement pastes. Powder Technol 2019;345:54–63. https://doi.org/10.1016/j.powtec.2018.12.094.
[28] Ma S, Qian Y, Kawashima S. Performance-based study on the rheological and hardened properties of blended cement mortars incorporating palygorskite clays and carbon nanotubes. Construct Build Mater 2018;171:663–71. https://doi.org/10.1016/j.conbuildmat.2018.03.121.
[29] Chindaprasirt P, Hatanaka S, Chareerat T, Mishima N, Yuasa Y. Cement paste characteristics and porous concrete properties. Construct Build Mater 2008;22:894–901. https://doi.org/10.1016/j.conbuildmat.2006.12.007.
[30] Hou S, Duan Z, Xiao J, Li L, Bai Y. Effect of moisture condition and brick content in recycled coarse aggregate on rheological properties of fresh concrete. J Build Eng 2021;35:102075. https://doi.org/10.1016/j.jobe.2020.102075.
[31] Nkinamubanzi P-C, Aïtcin P-C. Cement and superplasticizer combinations: compatibility and robustness. Cem Concr Aggregates 2004;26:1–8. https://doi.org/10.1520/CCA12329.
[32] Kevern JT, Biddle D, Cao Q. Effects of macrosynthetic fibers on pervious concrete properties. J Mater Civ Eng 2015;27:06014031. https://doi.org/10.1061/(ASCE)MT.1943-5533.0001213.
[33] Lian C, Zhuge Y, Beecham S. The relationship between porosity and strength for porous concrete. Construct Build Mater 2011;25:4294–8. https://doi.org/10.1016/j.conbuildmat.2011.05.005.
[34] Kumar R, Bhattacharjee B. Porosity, pore size distribution and in situ strength of concrete. Cement Concr Res 2003;33:155–64. https://doi.org/10.1016/S0008-8846(02)00942-0.
[35] Kim H, Hong J, Pyo S. Acoustic characteristics of sound absorbable high performance concrete. Appl Acoust 2018;138:171–8. https://doi.org/10.1016/j.apacoust.2018.04.002.
[36] Vikan H, Justnes H. Rheology of cementitious paste with silica fume or limestone. Cement Concr Res 2007;37:1512–7. https://doi.org/10.1016/j.cemconres.2007.08.012.
[37] Duan Z, Hou S, Xiao J, Singh A. Rheological properties of mortar containing recycled powders from construction and demolition wastes. Construct Build Mater 2020;237:117622. https://doi.org/10.1016/j.conbuildmat.2019.117622.
[38] Li L, Lu JX, Zhang B, Poon CS. Rheology behavior of one-part alkali activated slag/glass powder (AASG) pastes. Construct Build Mater 2020;258:120381. https://doi.org/10.1016/j.conbuildmat.2020.120381.
[39] Han Y, Yang Z, Ding T, Xiao J. Environmental and economic assessment on 3D printed buildings with recycled concrete. J Clean Prod 2021;278:123884. https://doi.org/10.1016/j.jclepro.2020.123884.